We are IntechOpen, the world's leading publisher of Open Access books Built by scientists, for scientists

6,900
Open access books available

185,000
International authors and editors

200M
Downloads

Our authors are among the

154
Countries delivered to

TOP 1%
most cited scientists

12.2%
Contributors from top 500 universities



WEB OF SCIENCE™

Selection of our books indexed in the Book Citation Index in Web of Science™ Core Collection (BKCI)

Interested in publishing with us?
Contact book.department@intechopen.com

Numbers displayed above are based on latest data collected.
For more information visit www.intechopen.com



Chapter

Improving Disturbance-Rejection by Using Disturbance Estimator

Damir Vrančić and Mikuláš Huba

IntechOpen

Abstract

The main tasks of control in various industries are either tracking the setpoint changes or rejecting the process disturbances. While both aim at maintaining the process output at the desired setpoint, the controller parameters optimised for setpoint tracking are generally not suitable for optimal disturbance rejection. The overall control performance can be improved to some extent by using simpler 2-DOF PID controllers. Such a controller structure allows the disturbance rejection to be optimised, while it also improves the setpoint tracking performance with additional controller parameters (usually through the setpoint weighting factors). Since such 2-DOF structures are usually relatively simple, the optimization of tracking performance is usually limited to the reduction of process overshoots instead of achieving an optimal (fast) tracking response. In this chapter, an alternative approach is presented in which the parameters of the PID controller are optimised for reference tracking, while the performance of the disturbance rejection is substantially increased by introducing a simple disturbance estimator approach. The mentioned estimator requires adding two simple blocks to the PID controller. The blocks are the second-order transfer functions whose parameters, including the PID controller parameters, can be calculated analytically from the process characteristic areas (also called process moments). The advantage of such an approach is that the mentioned areas can be analytically calculated directly from the process transfer function (of any order with time delay) or from the time response of the process when the steady state of the process is changed. Both of the above calculations are absolutely equivalent. Moreover, the output noise of the controller is under control as it is considered in the design of the controller and compensator. The closed loop results on several process models show that the proposed method with disturbance estimator has excellent tracking and disturbance rejection performance. The proposed controller structure and tuning method also compare favourably with some existing methods based on non-parametric description of the process.

Keywords: tuning method, disturbance rejection, disturbance estimator, multi-objective design

1. Introduction

The control of industrial processes requires efficient control loops. A majority of the control loops in various industries are implemented by the Proportional-Integrative-Derivative (PID) control algorithms. For efficient control, the PID controllers require proper tuning of the PID controller parameters. The parameters

can be calculated to optimise various performance criteria such as integral of error (IE), integral of absolute error (IAE), integral of squared error (ISE) and similar [1–4]. However, the most important decision that should be made in advance is the choice of the main purpose of the closed-loop system. Namely, the user should choose between the optimal closed-loop responses to reference changes (so-called tracking responses) or the optimal response to process disturbances. While there are many industrial processes that require optimal reference tracking responses, such as robot manipulation, welding, and batch processes, the majority of industrial processes require optimal disturbance rejection.

The history of tuning rules is long, originating in the 1940s with the famous Ziegler-Nichols tuning rules. In the following decades, many other tuning rules have been developed [1, 2, 4–10]. The rules can be generally categorised according to the required data of the process. The process can be described either in parametric form, e.g., as a process model (transfer function), or in nonparametric form, e.g., as a process time-response.

A relatively new tuning method that optimises either closed-loop tracking or disturbance rejection is the Magnitude-Optimum-Multiple-Integration (MOMI) method [7, 9, 11, 12]. The MOMI method is based on the Magnitude Optimum method, which aims to optimise the frequency response of the closed loop to achieve fast and stable closed loop time response [10, 13–15]. An interesting feature of the MOMI method is that it works either on the process given by its transfer function (of arbitrary order with time delay) or directly on the time response of the process during the steady state change. It is worth noting that both the parametric and non-parametric process data give exactly the same PID tuning results.

Many tuning methods for PID controllers provide different sets of controller parameters for tracking and disturbance rejection response. Similarly, the MOMI method primarily optimises the tracking response, while its modification, the Disturbance-Rejection-Magnitude-Optimum (DRMO) method, aims at optimising the disturbance rejection response. The latter significantly improves the disturbance rejection response, while the tracking response slows down due to the implemented reference-weighting gain or reference signal filter [9, 16, 17].

The main approach presented in this chapter is the alternative approach. First, the parameters of the PID controller are optimised for tracking performance. Then, a simple disturbance estimator is introduced to significantly increase the disturbance rejection performance [18, 19]. The advantages of the above approach are twofold. First, the disturbance rejection performance can significantly outperform that obtained by the DRMO method. Second, the parameters of the disturbance estimator can also be obtained directly from the non-parametric process data in the time domain. Therefore, the proposed approach can still be applied to the process data which is either in parametric or non-parametric form.

However, in practice, the process output noise is always present. If the controller or estimator gains are too high, the process input signals may be too noisy for practical applications. Therefore, noise attenuation should already be taken into account when calculating the controller and estimator parameters. This chapter shows how to achieve the best trade-off between performance and noise attenuation.

2. Process and controller description

The classic 1-degree-of-freedom (1-DOF) control loop configuration of the process and the controller is shown in **Figure 1**, where the signals r, e, u, d and y

DOI: http://dx.doi.org/10.5772/intechopen.95615

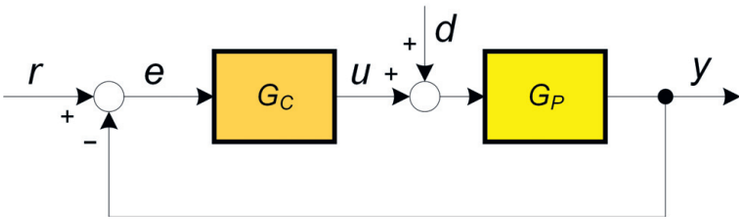


Figure 1.
The 1-DOF PID controller and the process in the closed-loop configuration.

represent the reference, the control error, the controller output, the process input disturbance, and the process output, respectively.

A process model (1) can be described by the following process transfer function:

$$G_P(s) = \frac{K_{PR}(1 + b_1 s + b_2 s^2 + \cdots + b_m s^m)}{1 + a_1 s + a_2 s^2 + \cdots + a_n s^n} e^{-sT_{del}} \tag{1}$$

where a_1 to a_n are the denominator coefficients, b_1 to b_m are the numerator coefficients, K_{PR} is the process gain, and T_{del} is the process time delay. Note that $n > m$ represents a strictly proper process transfer function and that the process is stable.

The PID controller is described by the following expression:

$$G_C(s) = \frac{K_I + K_P s + K_D s^2}{s(1 + sT_F)} \tag{2}$$

where K_I is the integrating gain, K_P is the proportional gain, and K_D is the derivative gain. Note that all three controller terms are filtered by the first-order filter with time constant T_F.

The closed-loop transfer function G_{CL} between the reference (r) and the process output (y) is as follows:

$$G_{CL} = \frac{G_C G_P}{1 + G_C G_P} \tag{3}$$

Since the structure of a 1-DOF PID controller does not provide optimal tracking and disturbance rejection at the same time, the 2-degrees-of-freedom (2-DOF) controller can be used instead [1, 2, 4, 8, 16, 20], where G_{CR} and G_{CY} denote the controller transfer function from the reference and the process output, respectively:

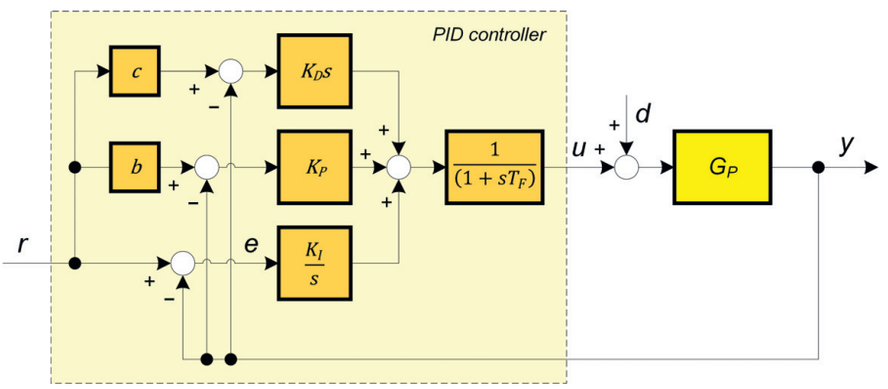


Figure 2.
The 2-DOF PID controller and process in the closed-loop configuration.

$$u = G_{CR}(s)r - G_{CY}(s)y$$
$$G_{CR} = \frac{K_I + bK_P s + cK_D s^2}{s(1 + sT_F)}$$
$$G_{CY} = \frac{K_I + K_P s + K_D s^2}{s(1 + sT_F)}, \tag{4}$$

as shown in **Figure 2**, where parameters b and c are reference-weighting parameters for the proportional and derivative terms, respectively.

3. MOMI and DRMO tuning methods

The MOMI and DRMO methods, as mentioned earlier, are based on the Magnitude Optimum (MO) method, which goes back to Whitley in 1946 [10]. The MO method shapes the closed-loop amplitude frequency response equal to one in a wide frequency range [6, 7, 10, 12–14, 21]. Such a closed-loop frequency response is usually "mirrored" into a fast and stable closed-loop time response.

The calculation of controller parameters has been simplified when using the MO method by determining the process characteristic areas or moments, which can be measured directly from the time responses during the change of the process steady-state [12, 15, 21, 22]. The mentioned areas or moments (A_1 to A_k) can also be calculated from the process model:

$$A_0 = K_{PR}$$
$$A_1 = K_{PR}(a_1 - b_1 + T_{del})$$
$$A_2 = K_{PR}\left[b_2 - a_2 - b_1 T_{del} + \frac{T_{del}^2}{2!}\right] + A_1 a_1$$
$$\vdots$$
$$A_k = K_{PR}\left[(-1)^{k+1}(a_k - b_k) + \sum_{i=1}^{k}(-1)^{k+i}\frac{T_{del}^i b_{k-i}}{i!}\right] + \sum_{i=1}^{k-1}(-1)^{k+i-1}A_i a_{k-i} \tag{5}$$

The controller parameters, for a given filter time constant T_F, are then calculated as follows:

$$\begin{bmatrix} K_I \\ K_P \\ K_D \end{bmatrix} = \begin{bmatrix} -A_1^* & A_0^* & 0 \\ -A_3^* & A_2^* & -A_1^* \\ -A_5^* & A_4^* & -A_3^* \end{bmatrix}^{-1} \begin{bmatrix} -0.5 \\ 0 \\ 0 \end{bmatrix}, \tag{6}$$

where the modified areas A_0^* to A_5^* are:

$$A_0^* = A_0$$
$$A_1^* = A_1 + A_0 T_F$$
$$A_2^* = A_2 + A_1 T_F + A_0 T_F^2$$
$$\vdots \tag{7}$$

The reference-weighting factors are $b = c = 1$. Note that the areas (moments) in expression (6) apply areas of the process including the controller filter G_F with time constant T_F (4):

$$G_F = \frac{1}{(1 + sT_F)} \tag{8}$$

by using expression (7) [9]. The aforementioned modification of the method, referred to as the MOMI method, allowed the controller parameters to be computed directly from the process time response [12, 21] or from the process transfer function.

Since the MOMI method aims at optimising the tracking performance, the disturbance rejection performance may be degraded for some types of processes.

To improve the disturbance-rejection performance, the optimisation criteria of the MOMI method were modified accordingly. The new method, referred to as the DRMO (Disturbance-Rejection-Magnitude-Optimum) method, achieved significantly improved disturbance rejection performance [9, 16, 17].

Similar to the MOMI method, the controller parameters in the DRMO method are also based on characteristic areas or moments. Therefore, the controller parameters can be calculated either from the process time-response or from the process transfer function.

The PID controller parameters are calculated according to the following expressions when using the DRMO method [9, 16, 17]:

$$K_P = \frac{\beta - \sqrt{\beta^2 - \alpha\gamma}}{\alpha}$$

$$K_I = \frac{\left(1 + K_P A_0^*\right)^2}{2\left(K_D A_0^{*2} + A_1^*\right)} \tag{9}$$

where

$$\alpha = A_1^{*3} + A_0^{*2} A_3^* - 2A_0^* A_1^* A_2^*$$

$$\beta = A_1^* A_2^* - A_0^* A_3^* + 2K_D\left(A_0^* A_1^{*2} - A_0^{*2} A_2^*\right)$$

$$\gamma = K_D^3 A_0^{*4} + 3K_D^2 A_0^{*2} A_1^* + K_D\left(2A_0^* A_2^* + A_1^{*2}\right) + A_3^* \tag{10}$$

and the derivative gain K_D is calculated directly from expression (6). The reference-weighting factors are $b = c = 0$.

The DRMO tuning method significantly improved the disturbance rejection performance, especially for the lower-order processes. However, the reference tracking becomes slower due to the reference-weighting factors $b = c = 0$ in the 2-DOF control structure (4). The problem can be circumvented by including a simple disturbance estimator in the control scheme. Such a solution is denoted as DE-MOMI method.

4. DE-MOMI tuning method

In order to improve the disturbance rejection response, while retaining the tracking response obtained by the MOMI method, a disturbance estimator has been added to the PID controller $G_C(s)$ (2), as depicted in **Figure 3**.

The disturbance estimator consists of the process model G_M, the inverse process model G_{MI} and the filter G_{FD}. In hypothetical case, when the process model is ideal representation of the bi-proper process without time-delay, and the filter $G_{FD} = 1$:

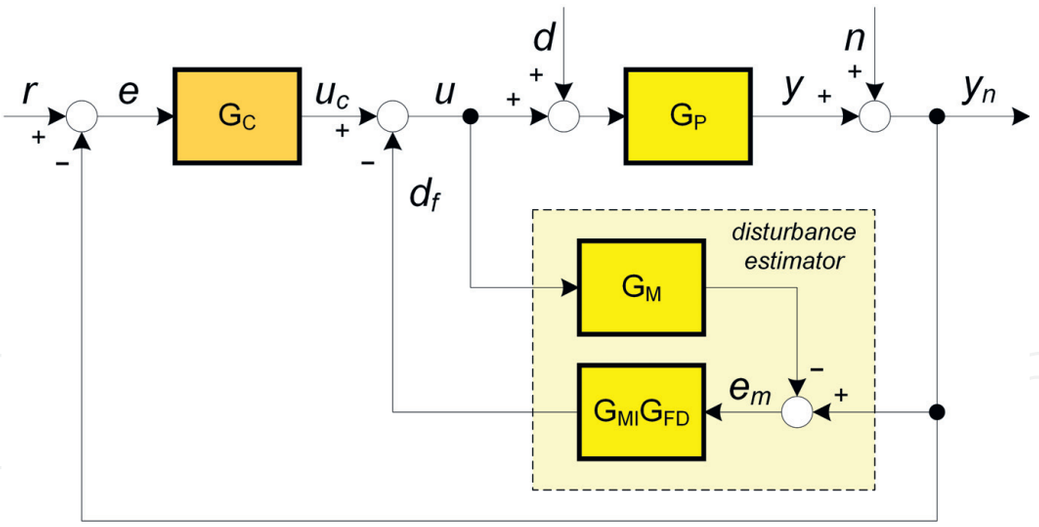


Figure 3.
The PID controller with disturbance estimator.

$$G_M = G_P, G_{MI} = G_M^{-1}, G_{FD} = 1, \tag{11}$$

the estimated disturbance d_f equals to the actual disturbance d:

$$d_f = d. \tag{12}$$

In this case the ideal disturbance compensation is achieved. However, in practice, model mismatch may occur (due to changing process characteristics in time or working point, lower-order process model or the process non-linearity), and the inverse of the process usually cannot be obtained, since majority of the actual processes are either strictly proper or they have time delays. Therefore, another strategy is required.

For practical applications, the solution has to be as simple as possible. In this manner we decided to use the following process model, the inverse process model and the disturbance estimator filter:

$$\begin{aligned} G_M &= \frac{K_{PRM} e^{-sT_{delm}}}{1 + a_{1m}s + a_{2m}s^2} \\ G_{MI} &= \frac{1 + a_{1m}s + a_{2m}s^2}{K_{PRM}} \\ G_{FD} &= \frac{K_{FD}}{(1 + sT_{FD})^3} \end{aligned} \tag{13}$$

where K_{PRM} and T_{delm} are the process model gain and time delay and a_{1m} and a_{2m} are the process model dynamic parameters. Parameters K_{FD} and T_{FD} are the disturbance filter gain and time constant, respectively.

The remaining question is how to obtain the process model if the actual process is of the higher order or if the actual process is not known (e.g. the areas (moments) were calculated directly from the process time-response)? Fortunately, the process model can be calculated directly from the obtained areas (5), as derived in [23]:

$$\frac{T_{delm}^3}{6} - \frac{A_1}{2A_0} T_{delm}^2 + \left(\frac{A_1^2}{A_0^2} - \frac{A_2}{A_0} \right) T_{delm} + \frac{2A_1A_2}{A_0^2} - \frac{A_3}{A_0} - \frac{A_1^3}{A_0^3} = 0$$

$$K_{PRM} = A_0$$

$$a_{1m} = \frac{A_1}{A_0} - T_{delm}$$

$$a_{2m} = -\frac{A_2}{A_0} + \frac{a_{1m}A_1}{A_0} + \frac{T_{delm}^2}{2} \tag{14}$$

The process model delay T_{delm} is calculated from the third-order equation in (14). The solution is the smallest real positive result [23].

Now, all the model parameters are known and the disturbance filter G_{FD} parameters should be derived. Before continuing the derivation we should be aware of the fact that $G_{MI}(s)$ is not proper, so it cannot be realised in practice without the accompanied filter $G_{FD}(s)$. Multiplication of both is strictly proper, so the entire block can be easily implemented inside the controller.

Derivation of disturbance filter parameters depends mainly on desired disturbance rejection performance. It is natural that the disturbance signal reconstruction (d_f) is faster if the filter time constant T_{FD} is smaller. In hypothetical case, if $G_M = G_P$, the reconstructed disturbance signal d_f becomes:

$$d_f = K_{FD}\frac{e^{-sT_{delm}}}{(1+sT_{FD})^3}d \tag{15}$$

With sufficiently small time constant ($T_{FD} \to 0$), where the disturbance filter gain $K_{FD} = 1$, and there is no process time delay, $df \approx d$. In this case the reconstructed disturbance signal d_f perfectly compensates the disturbance d. On the other hand, smaller disturbance filter time constant significantly increases the process output noise present in the measurements and forwards it to the controller output. Therefore, the T_{FD} should be selected according to the tolerated noise gain of the disturbance estimator, as will be discussed in detail in the next sub-chapter.

One remaining parameter of the disturbance filter G_{FD} (13) is the gain K_{FD}. One would, naturally, expect that the most optimal value should be $K_{FD} = 1$, since only in this case, after some time, d_f becomes the same to d (15). Therefore, the process input disturbance d is eliminated by the reconstructed disturbance d_f. However, as will be shown below, the optimal disturbance response is obtained with lower values of the gain K_{FD}. Namely, due to the disturbance compensator, the external process input signal d generates the delayed reconstructed disturbance signal d_f (15). Combined together, the actual process input u, due to disturbance d, is d-d_f. The step-like signal d, therefore, generates pulse-like actual process input disturbance signal d-d_f. Since the PID controller is present in the loop, and it contains the integrating term, the process output (y) deviation in one direction (e.g. above the reference) should be compensated by the process output deviation in the opposite direction (e.g. below the reference). Namely, when using $K_{FD} = 1$, the integral of the control error must be:

$$\int_{t=0}^{\infty} e(t)dt = 0. \tag{16}$$

It means that, by applying $K_{FD} = 1$, the additional process undershoot, after the initial process overshoot due to the disturbance d, is inevitable.

Figure 4 shows an example on delayed second-order process, when applying the step-wise external process input disturbance signal d, and when using $K_{FD} = 1$ (upper figure) and $K_{FD} = 0.44$ (lower figure). The process output undershoot in the upper figure is clearly seen. By appropriately reducing the filter gain to $K_{FD} = 0.44$, the disturbance rejection response is improved (lower figure).

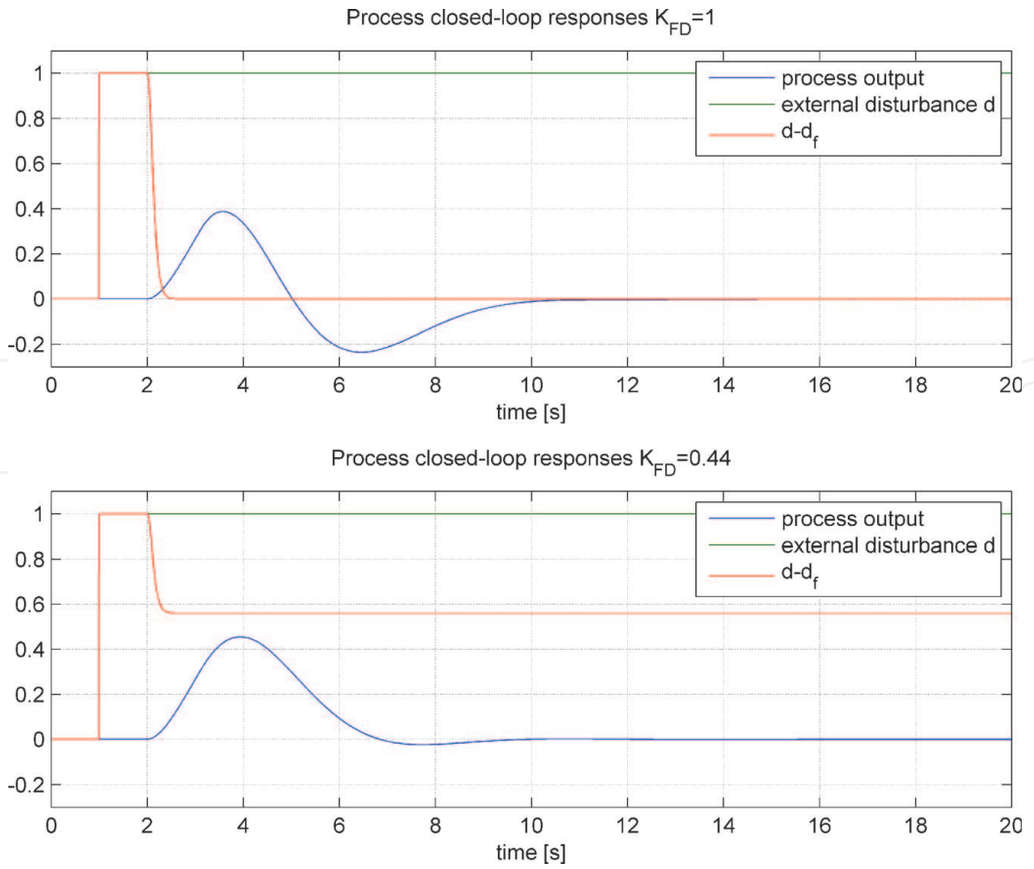


Figure 4.
The closed-loop signals when applying step-wise external process input disturbance signal with disturbance filter gains K_{FD} *= 1 (upper figure) and* K_{FD} *= 0.44 (lower figure).*

The remaining question is how to find the most appropriate filter gain K_{FD}. Certainly, the K_{FD} should be chosen so as that the disturbance rejection is optimised. Here we can use the same optimisation criteria as in the DRMO tuning method. Therefore, the transfer function $G_{CLD}(s)$ between the external disturbance (d) and the process output (y):

$$G_{CLD}(s) = \frac{Y(s)}{D(s)} = \frac{G_M\left(1 - G_{FD}e^{-sT_{delm}}\right)}{1 + G_M G_P} \tag{17}$$

should be optimised according to the modified MO criterion [9, 16]. Note that expression (17) holds when the process and the model transfer functions are equivalent. Since the disturbance filter time constant is defined, and all of the controller and the model parameters are calculated, the only optimisation parameter is the gain K_{FD}. By using similar derivation as in [9, 16], the optimal filter gain K_{FD} is calculated as:

$$K_{FD} = \frac{-b_0 + \sqrt{b_0^2 - 4a_0c_0}}{2a_0} \tag{18}$$

where

$$a_0 = -d_0 + 2f_0K_{IP} + K_{IP}^2\left(T_F^2 - 3T_{FD}^2\right)$$
$$b_0 = 2d_0 - 4f_0K_{IP} + K_{IP}^2\left(-2T_F^2 + 12T_{FD}^2 + 6T_{FD}T_{delm} + T_{delm}^2\right)$$
$$c_0 = -d_0 + 2f_0K_{IP} + K_{IP}^2T_F^2$$

$$K_{IP} = K_I K_{PRM}$$
$$K_{PP} = K_P K_{PRM}$$
$$K_{DP} = K_D K_{PRM}$$
$$d_0 = (1 + K_{PP})^2$$
$$f_0 = a_{1m} + K_{DP} + T_F + T_{delm} \tag{19}$$

For the given controller filter (T_F) and the disturbance filter (T_{FD}) time constants (note that the calculation of both time constants, according to the desired level of noise, will be derived in the next sub-chapter), the calculation of remaining controller, model and disturbance filter parameters proceeds as given in **Figure 5**.

Illustrative example 1

To illustrate the proposed design of DE-MOMI method, according to control structure in **Figure 5**, let us calculate the controller, model and disturbance filter parameters for the following processes:

$$G_{P1} = \frac{e^{-0.5s}}{(1+s)^2}$$
$$G_{P2} = \frac{e^{-0.2s}}{(1+s)^3} \tag{20}$$

The a-priori chosen filter time constants were:

$$T_F = T_{FD} = 0.1 \tag{21}$$

The characteristic areas, calculated from (5) and (7), are given in **Table 1**.

Next, the PID controller parameters are calculated from (6) and from (9), since we are going to compare the proposed DE-MOMI method with MOMI and DRMO methods. The calculated controller parameters are given in **Table 2**.

The process models G_M and inverse process models G_{MI} are then calculated from (14), where G_{MI} is the inverse of G_M without time-delay:

1. Calculate the characteristic areas or moments from the process time-response [9,12] or from (5) if the process transfer function is known in advance.
2. Calculate modified areas according to the chosen T_F from (7).
3. Calculate PID controller parameters from (6).
4. Calculate process model parameters from (14).
5. Calculate the disturbance filter gain K_{FD} from (18).

Figure 5.
Calculation of the controller, model and filter parameters.

	A_0	A_1	A_2	A_3	A_4	A_5
Areas G_{P1}	1	2.50	4.13	5.77	7.42	9.07
Areas G_{P1} with controller filter	1	2.60	4.39	6.21	8.04	9.87
Areas G_{P2}	1	3.20	6.62	11.26	17.12	24.21
Areas G_{P2} with controller filter	1	3.30	6.95	11.96	18.32	26.04

Table 1.
The calculated areas for the processes (20) without and with the controller filter.

Controller parameters	K_P	K_I	K_D
MOMI controller for G_{P1}	1.81	0.89	0.93
DRMO controller for G_{P1}	2.25	1.49	0.93
MOMI controller for G_{P2}	1.61	0.64	1.08
DRMO controller for G_{P2}	1.93	0.98	1.08

Table 2.
The calculated controller parameters for the processes (20) for MOMI (6) and DRMO (9) method, taking into account the chosen controller filter T_F = 0.1.

$$G_{M1} = \frac{e^{-0.5s}}{1 + 2s + s^2}$$
$$G_{MI1} = 1 + 2s + s^2$$
$$G_{M2} = \frac{e^{-0.616s}}{1 + 2.58s + 1.84s^2} \tag{22}$$
$$G_{MI2} = 1 + 2.58s + 1.84s^2$$

Finally, the disturbance filter gain K_{FD}, when taking into account the chosen T_{FD} = 0.1, is then calculated from (18):

$$K_{FD1} = 0.57$$
$$K_{FD2} = 0.59 \tag{23}$$

Therefore, the complete inverse of the models with accompanying disturbance filters (see **Figure 3**) are the following:

$$G_{MI1}G_{FD1} = \frac{0.57(1 + 2s + s^2)}{(1 + 0.1s)^3}$$
$$G_{MI2}G_{FD2} = \frac{0.59(1 + 2.58s + 1.84s^2)}{(1 + 0.1s)^3} \tag{24}$$

The closed-loop responses, obtained with the calculated controller, model and filter parameters, for the MOMI, DRMO and the proposed DE-MOMI method, are given in **Figures 6** and 7. At t = 0 s, the reference value (r) was changed from 0 to 1 and at half of experiment time the process input disturbance (d) was changed from 0 to 1. It is obvious that the disturbance rejection performance of the DE-MOMI method is the best. Note that when applying the DE-MOMI method, due to the difference between the actual process and the process model in the second example (G_{P2}), the process input signal, during the reference change, is not smooth. This is expected, since the inverse process model with filter is amplifying the difference between the actual process and the process model. In this case, the response can be made smoother by increasing the disturbance filter time constant (T_{FD}). Note that a possible limitation of the control signal can also help to smooth out the oscillations after the reference step [24].

The disturbance rejection performance of the DE-MOMI method can be increased by decreasing the disturbance filter time constant T_{FD}. However, as already mentioned above, the process input signal can become oscillatory when the actual process and the process model differ. In this case, too small T_{FD} can even render the closed-loop system unstable. Besides that, the process noise (signal n in

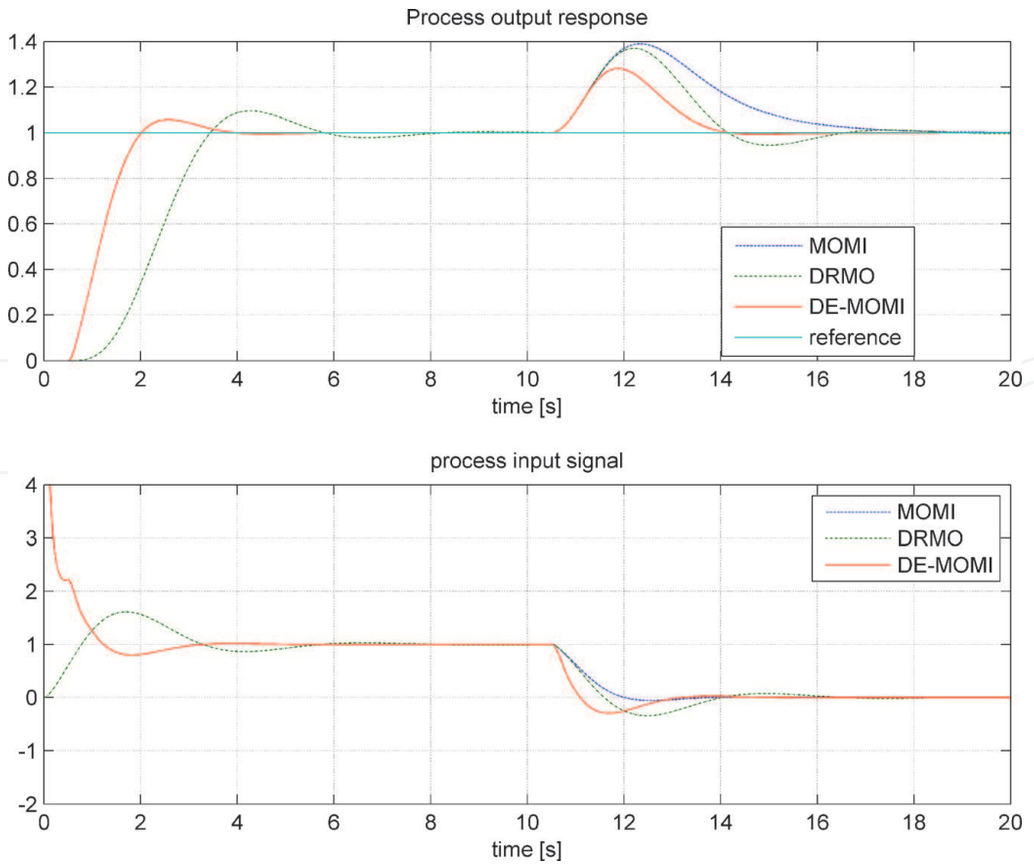


Figure 6.
The closed-loop responses on the process G_{P1}, when using the MOMI, DRMO and DE-MOMI method.

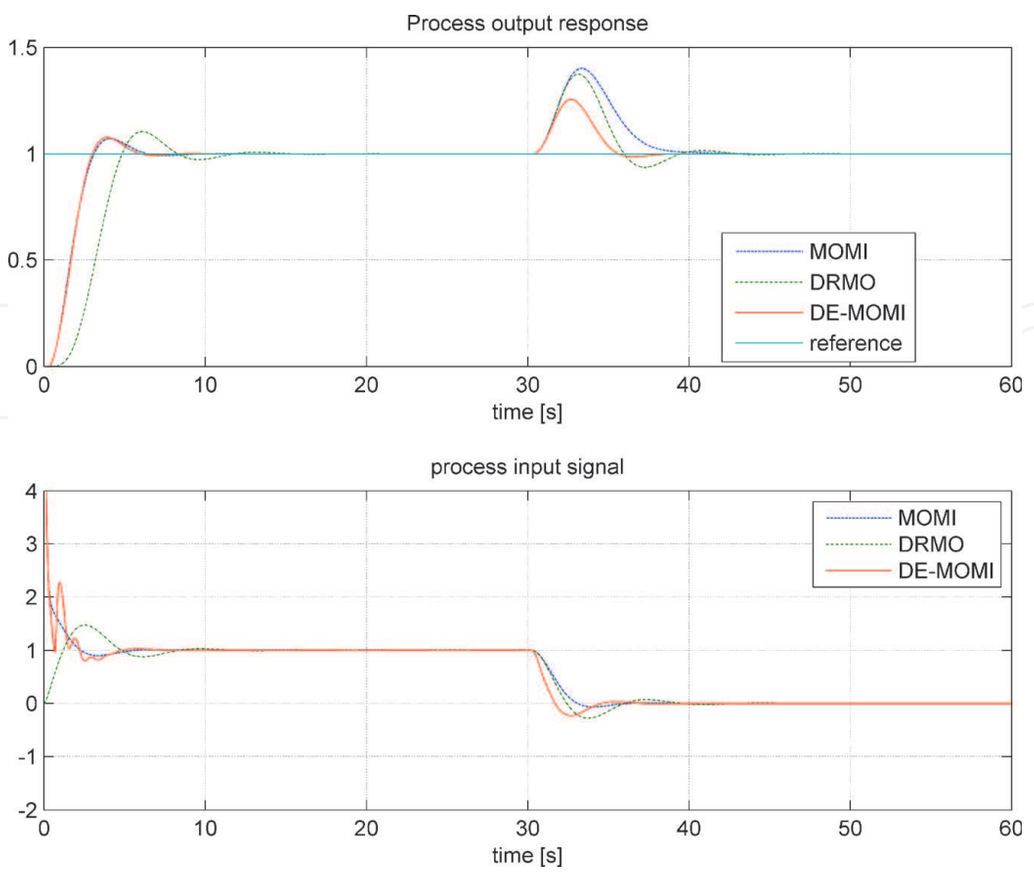


Figure 7.
The closed-loop responses on the process G_{P2}, when using the MOMI, DRMO and DE-MOMI method.

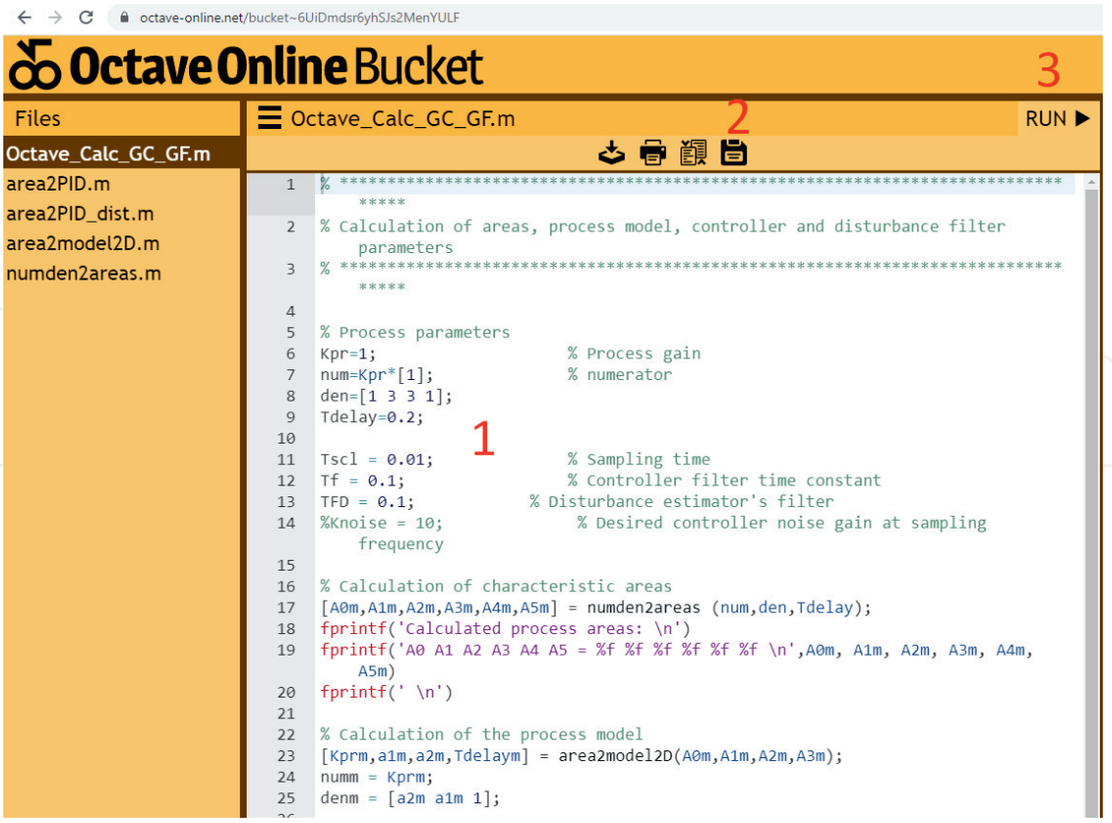


Figure 8.
The website layout for the calculation of the controller and the DE parameters.

Figure 3) is also amplified via block $G_{MI}G_{FD}$, so small T_{FD} can cause excessive noise of signal d_F. The selection of T_{FD} is, therefore, important in practical realisation of the DE-MOMI method.

Calculating the controller and DE parameters is a relatively simple process. However, to simplify it even further, all Matlab/Octave scripts are available on the OctaveOnline Bucket website [25]. The layout of the website is shown in **Figure 8**. To calculate the controller and DE parameters, the user must 1) change the process and filter parameters, 2) press the "Save" button, and 3) press the "Run" button. The script will be executed and on the right side of the web screen all calculated parameters will be displayed. Note that users can change the content of the script only temporarily.

5. Noise attenuation of DE-MOMI method

As already mentioned in the previous sub-chapter, the output noise of disturbance estimator (d_F) depends on the selection of disturbance filter T_{FD}. However, according to **Figure 3**, some noise is also present at the output of the PID controller block (signal u_C). In this sub-chapter we will give some guidelines regarding the noise attenuation in practical realisation of DE-MOMI controller.

In practice, it is important to keep the controller output noise within some limits. Namely, if the controller's and the estimator's filter time constants are too low, the DE-MOMI controller output noise can be so high that the controller would be useless in practice.

The controller noise is mainly caused by the process output noise n (see **Figure 3**). The noise power at the controller output (u) depends on the power of

measurement noise n and the frequency properties of noise, PID controller and disturbance estimator. The relation between the filters (T_F and T_{FD}) time constants and the controller output noise is rather complex, but can be calculated according to Parseval's theorem if the measurement noise frequency characteristics are known. However, this relation is higher-order and non-linear. Therefore, the search for adequate filter time constants T_F and T_{FD} would require optimisation procedure, which would significantly complicate the otherwise simple method.

In practice, on the other side, it is enough to keep the noise sufficiently low at some sufficiently high frequency. The definition of "high frequency" is arguable. In discrete-realisation of the controller, the sampling frequency is

$$f_S = \frac{1}{T_S} \tag{25}$$

where T_S is the controller's sampling time. The highest signal, which may be sent to discrete function is, due to Shannon's theorem, $f_S/2$. Therefore, any frequency close to $f_S/2$ can be considered as high frequency. In this research we have arbitrarily decided that the "high frequency" f_{HF} is the quarter of controller's sampling frequency f_S:

$$\begin{aligned} f_{HF} &= 0.25 f_S \\ \omega_{HF} &= 2\pi f_{HF} = \frac{0.5\pi}{T_S} \end{aligned} \tag{26}$$

As already mentioned above, the source of controller noise is the process output noise n (**Figure 3**). In DE-MOMI controller, the overall high-frequency control noise consists of the PID controller (u_{PIDn}) and the disturbance estimator (u_{DEn}) high-frequency noise:

$$\begin{aligned} u_{PIDn}(\omega_{HF}) &= K_{PIDn} n(\omega_{HF}) \\ u_{DEn}(\omega_{HF}) &= K_{DEn} n(\omega_{HF}), \end{aligned} \tag{27}$$

where K_{PIDn} and K_{DEn} are the high-frequency gains (around frequency ω_{HF}) of the PID controller and the disturbance estimator, respectively.

In practical applications of the DE-MOMI method, the noise specifications (limitations) should be given in as simple form as possible for the user (operator). We decided that the actual parameters, given by the user should be the high-frequency gains of the controller (K_{PIDn}) and the disturbance estimator (K_{DEn}). Therefore, in practice, by selecting the mentioned two gains, the user would limit the amount of controller noise at high frequencies.

The actual gain of the PID controller around the chosen high frequency ω_{HF} can be calculated from the controller transfer function (2):

$$K_{PIDn} = \frac{\sqrt{\left(K_I - K_D \omega_{HF}^2\right)^2 + K_P^2 \omega_{HF}^2}}{\omega_{HF} \sqrt{1 + T_F^2 \omega_{HF}^2}} \tag{28}$$

The controller filter time constant can then be calculated as:

$$T_F = \frac{\sqrt{\omega_{HF}^4 K_D^2 + \omega_{HF}^2 \left(K_P^2 - 2K_I K_D - K_{PIDn}^2\right) + K_I^2}}{\omega_{HF}^2 K_{PIDn}} \tag{29}$$

Since the PID controller parameters depend on the filter time constant T_F, the T_F should be calculated by an iterative procedure given in **Figure 9**.

The calculation of the disturbance filter high-frequency gain K_{DEn} is similar as for the PID controller:

$$K_{DEn} = \sqrt{\frac{K_{FD}^2\left(1+\omega_{HF}^2\left(a_{1m}^2-2a_{2m}\right)+\omega_{HF}^4 a_{2m}^2\right)}{K_{PRM}^2\left(1+\omega_{HF}^2 T_{FD}^2\right)^3}} \tag{30}$$

In a similar manner, the disturbance filter time constant can be derived as:

$$T_{FD} = \frac{1}{\omega_{HF}}\sqrt{\sqrt[3]{\frac{K_{FD}^2\left(1+\omega_{HF}^2\left(a_{1m}^2-2a_{2m}\right)+\omega_{HF}^4 a_{2m}^2\right)}{K_{PRM}^2 K_{DEn}^2}}-1} \tag{31}$$

Since the calculated filter gain K_{FD} depends on the filter time constant T_{FD} (see expression (18)), the calculation of expression (31) is iterative as well, as given in **Figure 10**.

Illustrative example 2

Let us illustrate the calculation procedure for the following processes:

$$G_{P3} = \frac{e^{-0.2s}}{(1+0.2s)(1+s)}$$

$$G_{P4} = \frac{e^{-s}}{(1+s)^4} \tag{32}$$

Note that other process models were chosen as in the previous case (20) in order to test different types of processes. The chosen high-frequency gains of the PID controller and the disturbance filter are K_{PIDn} = 4 and K_{DEn} = 4, respectively. The chosen closed-loop sampling time was T_S = 0.01 s. Therefore, the chosen high-frequency is:

$$\omega_{HF} = \frac{0.5\pi}{T_S} = 157.1\,s^{-1} \tag{33}$$

1. Set the controller filter time constant to T_F=0 or to some small value.
2. Calculate the PID controller parameters from (6).
3. Calculate T_F from (29), according to the desired high-frequency gain K_{PIDn}.
4. Repeat steps 2 and 3 few times (about 2-3 iterations are usually sufficient)

Figure 9.
Calculation of the filter and controller parameters according to the desired controller high-frequency gain K_{PIDn}.

1. Set the controller filter time constant to T_{FD}=0 or to some small value.
2. Calculate the K_{FD} gain from (18).
3. Calculate T_{FD} from (31), according to the desired high-frequency gain K_{DEn}.
4. Repeat steps 2 and 3 few times (about 2-3 iterations are usually sufficient)

Figure 10.
Calculation of the disturbance filter parameters according to the desired disturbance filter high-frequency gain K_{DEn}.

The initially chosen filter time constants were (the values are not critical):

$$T_F = T_{FD} = 0.1\,s \tag{34}$$

The characteristic areas are calculated from (5). For the given high-frequency gain K_{PIDn} = 4, the filter and controller parameters are calculated according to procedure given in **Figure 9**. The calculated filter time constants (after 2 iterations) were

$$\begin{aligned} T_{F3} &= 0.119\,s \\ T_{F4} &= 0.192\,s \end{aligned} \tag{35}$$

Note that indexes 3 and 4 in above filter time constants stand for the processes G_{P3} and G_{P4}, respectively.

The areas are given in **Table 3** and the controller parameters are given in **Table 4**.

The process models G_M and inversed process models G_{MI} are then calculated from (14):

$$\begin{aligned} G_{M3} &= \frac{e^{-0.2s}}{1 + 1.2s + 0.2s^2} \\ G_{MI3} &= 1 + 1.2s + 0.2s^2 \\ G_{M4} &= \frac{e^{-1.94s}}{1 + 3.06s + 2.69s^2} \\ G_{MI4} &= 1 + 3.06s + 2.69s^2 \end{aligned} \tag{36}$$

According to the chosen high-frequency gain K_{DEn} = 4, the T_{FD} and K_{FD} were calculated according to the procedure given in **Figure 10** (2 iterations were sufficient):

$$\begin{aligned} T_{FD3} &= 0.06 \\ T_{FD4} &= 0.116 \\ K_{FD3} &= 0.69 \\ K_{FD4} &= 0.36 \end{aligned} \tag{37}$$

Therefore, the complete inverse of the models with accompanying disturbance filters (see **Figure 3**) are the following:

$$G_{MI3}G_{FD3} = \frac{0.69(1 + 1.2s + 0.2s^2)}{(1 + 0.06s)^3}$$

	A_0	A_1	A_2	A_3	A_4	A_5
Areas G_{P3}	1	1.40	1.50	1.52	1.53	1.53
Areas G_{P3} with controller filter	1	1.52	1.68	1.72	1.73	1.73
Areas G_{P4}	1	5.00	14.50	32.17	60.71	102.8
Areas G_{P4} with controller filter	1	5.19	15.50	35.14	67.45	115.8

Table 3.
The calculated areas for the processes (32) without and with the controller filter.

Controller parameters	K_P	K_I	K_D
MOMI controller for G_{P3}	2.35	1.88	0.48
DRMO controller for G_{P3}	2.91	3.83	0.48
MOMI controller for G_{P4}	0.84	0.26	0.77
DRMO controller for G_{P4}	0.94	0.32	0.77

Table 4.
The calculated controller parameters for the processes (20) for MOMI (6) and DRMO (9) method, taking into account the calculated controller filters.

$$G_{MI4}G_{FD4} = \frac{0.36(1 + 3.06s + 2.69s^2)}{(1 + 0.116s)^3} \tag{38}$$

The closed-loop responses for the MOMI, DRMO and the proposed DE-MOMI method, are given in **Figures 11** and **12**. Again, the disturbance rejection performance of the DE-MOMI method is the best (note that the unity-step process input disturbance signal was applied at the half of experiment time). The level of controller output (u) noise is close to the expected one taken into account that both, the PID controller (u_C) and the disturbance estimator output (d_F) noise should be 4-times higher than the measurement noise at high frequencies.

The disturbance rejection performance of the DE-MOMI method can be additionally improved by increasing the high-frequency gain K_{DEn}. However, increased gain is associated with higher controller output noise and decreased closed-loop stability if the actual process and the process model differ.

The computation of the controller and the DE parameters can be performed similarly as before on another OctaveOnline Bucket website [26]. The calculation of

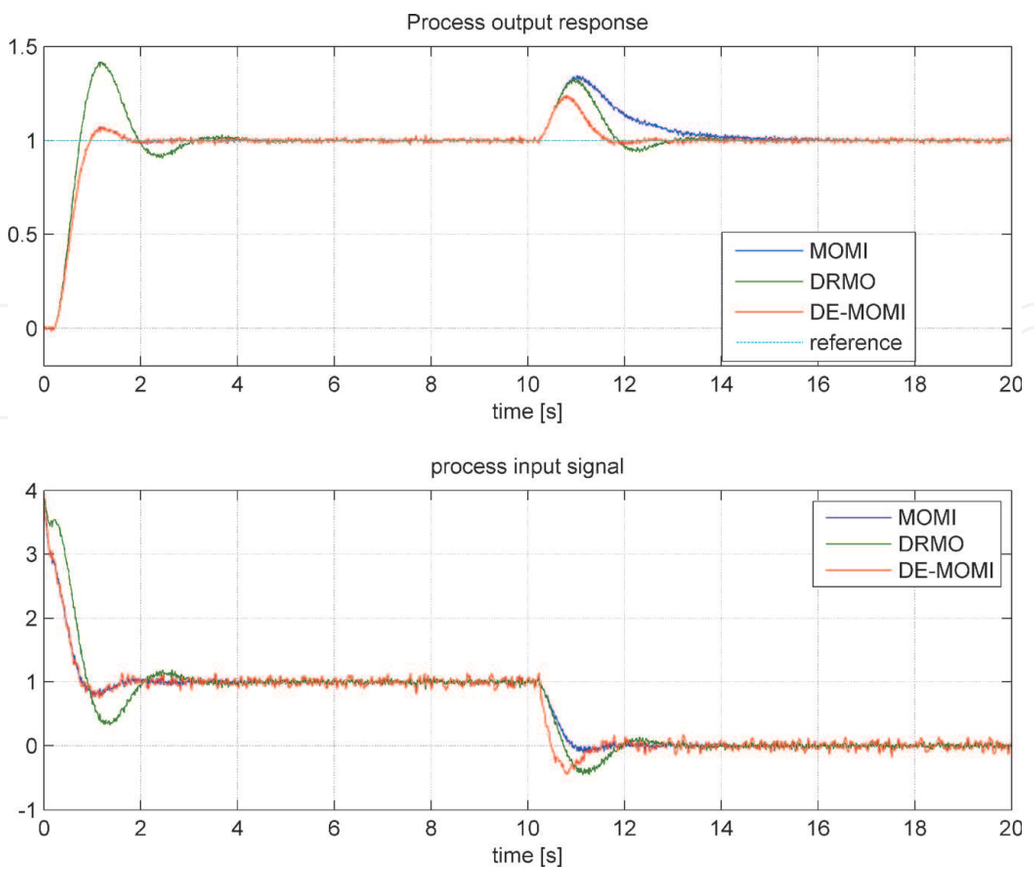


Figure 11.
The closed-loop responses on the process G_{P3}*, when using the MOMI, DRMO and DE-MOMI method.*

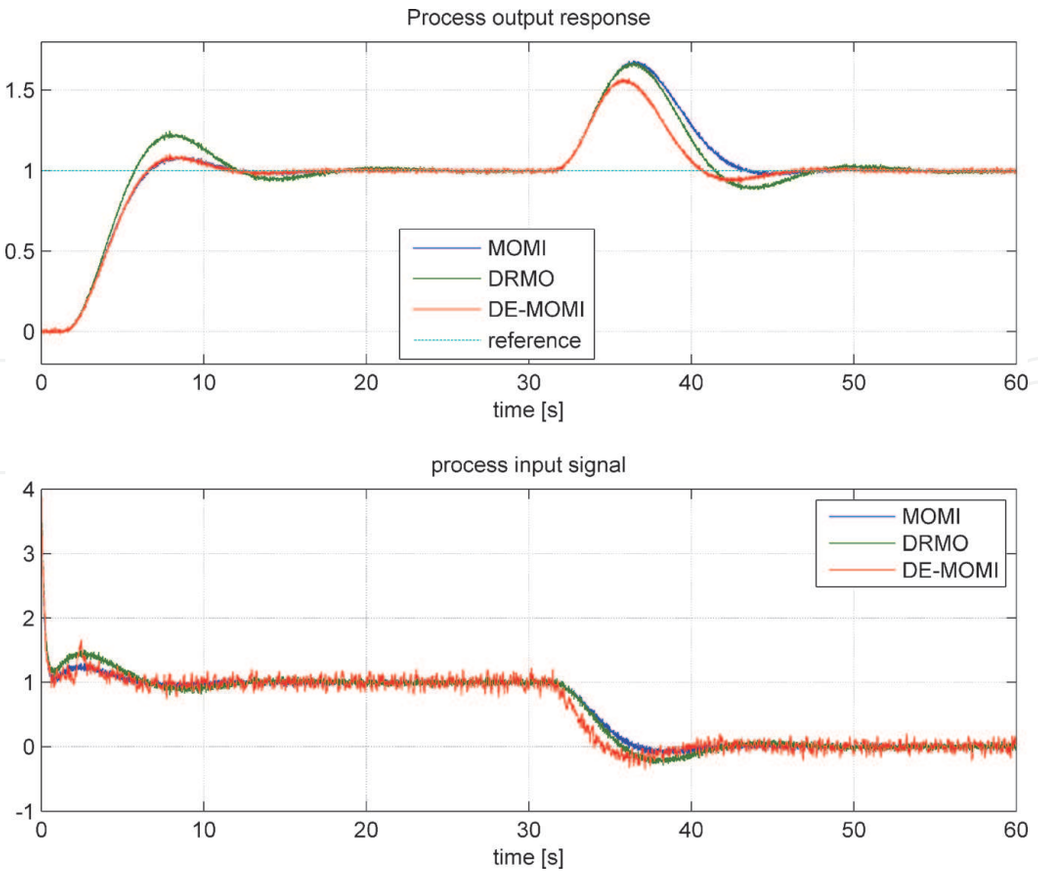


Figure 12.
The closed-loop responses on the process G_{P4}, *when using the MOMI, DRMO and DE-MOMI method.*

the parameters can be performed similarly as shown in **Figure 8**, with the difference that the name of the script is now Octave_Calc_GC_GF_Noise.m. To calculate the controller and DE parameters, the user must 1) change the process and noise gain parameters, 2) press the "Save" button, and then 3) press the "Run" button. The script will run and the right side of the web screen will display all the calculated parameters. Note that users can only temporarily change the contents of the script.

6. Comparison to some other methods

In this sub-chapter the proposed method will be compared to some other tuning methods based on non-parametric description of the process. Besides the already introduced MOMI and DRMO methods, the DE-MOMI method will be compared to Åström and Hägglund's tuning method [1] (denoted as "AH") and to ADRC method [27].

The AH method [1] is based on the calculation of the maximum sensitivity index M_S, which is the inverse of the smallest open-loop Nyquist curve distance to the critical point (−1,0i). The method was developed for values M_S = 1.4 and M_S = 2. In this comparison we will use M_S = 2, since it gives better disturbance-rejection performance. However, even though the process transfer function does not need to be derived, the method requires the identification of the process steady-state gain and the inflexion point along with maximum slope of the process output signal during the step-change of the process input signal. Note that those parameters usually require manual measurements and cannot be easily performed by using automatic calculation. The AH method is using the PID controller structure with adjustable reference-weighting factor b, and by fixing factor c = 0 (**Figure 2**).

The ADRC method [27–31] is based on a simple controller with three gains associated with extended state-observer (ESO), as shown in **Figure 13**.

The method does not require the process transfer function. However, few user-defined parameters, like the observer speed, the desired settling time and the main controller gain K_C, should be defined by the user before calculating the rest of ADRC parameters. As shown in **Figure 13**, the ADRC method is using control structure which consists of an extended state observer (ESO) with three gains (β_1, β_2 and β_3) and three controller gains (K_C, K_P and K_D) [27].

Since ADRC method depends on three user-defined parameters, which, in great extent, determine the closed-loop performance, we were limited to the set of processes tested in [27]. Someone would argue that, by limiting our choice to the mentioned processes, we are favouring the ADRC method. However, it should be noted that in [27], the ADRC method was tested on 8 different processes, so the choice of processes was actually not significantly limited. In this regard, the following two processes have been selected:

$$G_{P5} = \frac{1}{(1+s)(1+0.2s)(1+0.04s)(1+0.008s)}$$

$$G_{P6} = \frac{e^{-5s}}{(1+s)^3} \tag{39}$$

The PID controller parameters for the MOMI, DRMO, DE-MOMI and AH methods are given in **Tables 5** and **6**. The ADRC controller parameters are given in **Table 7**. The chosen high frequency gains for the PID controller and disturbance estimator are $K_{PIDn} = K_{DEn} = 20$ for G_{P5} and $K_{PIDn} = K_{DEn} = 4$ for G_{P6}. The higher gains were chosen for G_{P5}, since the closed-loop tracking and control performance was substantially improved when using higher gains. Increasing the gains for G_{P6} above 4 did not significantly improve the performance.

The sampling time for G_{P5} is chosen as $T_S = 0.001$ s and for G_{P6} as $T_S = 0.01$ s.

The closed-loop process responses are given in **Figures 14** and **15**. In both experiments the unity-step process input disturbance signal was applied at the half of experiment time.

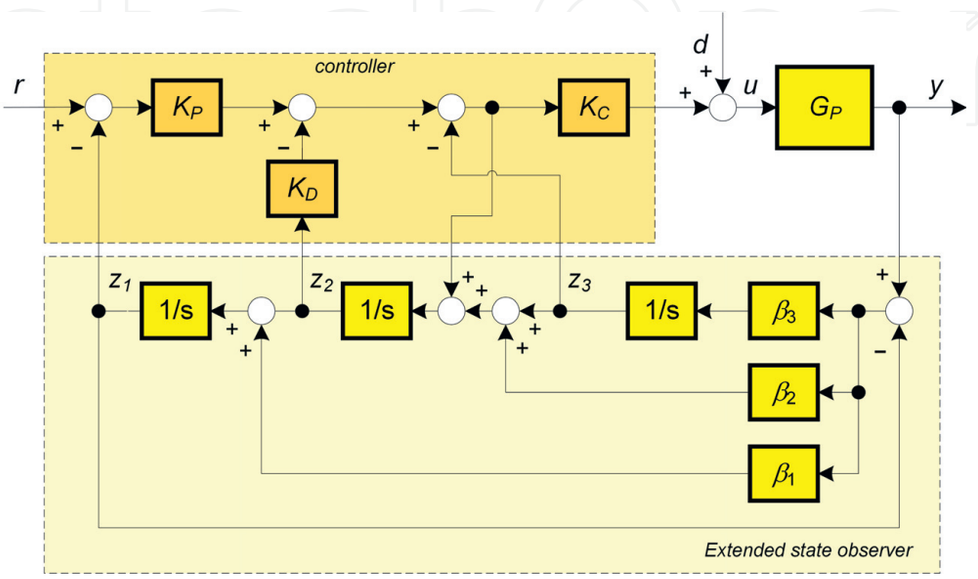


Figure 13.
The ADRC control structure with the controller gains (up) and the extended state observer (down).

Process	Tuning method	K_P	K_I	K_D	T_F	b	c
G_{P5}	MOMI	6.45	5.35	1.108	0.055	1	1
	DRMO	9.69	23.71	1.108	0.055	0	0
	DE-MOMI	6.45	5.35	1.108	0.055	1	1
	AH	21.35	53.05	2.22	0.055	0.24	0
G_{P6}	MOMI	0.53	0.126	0.66	0.165	1	1
	DRMO	0.57	0.140	0.66	0.165	0	0
	DE-MOMI	0.53	0.126	0.66	0.165	1	1
	AH	0.52	0.136	0.52	0.165	0.36	0

Table 5.
The calculated controller parameters for the processes (39) for MOMI, DRMO, DE-MOMI and AH method.

Process	K_{PRM}	a_{1m}	a_{2m}	T_{delm}	T_{FD}	K_{FD}
G_{P5}	1	1.205	0.205	0.043	0.018	0.909
G_{P6}	1	2.58	1.84	5.42	0.077	0.159

Table 6.
The calculated disturbance estimator's parameters for the processes (39) for DE-MOMI method.

Process	K_C	K_P	K_D	β_1	β_2	β_3
G_{P5}	1/5	100	20	120	4800	19200
G_{P6}	1/3	0.16	0.8	4.8	7.68	30.72

Table 7.
The calculated ADRC controller parameters for the processes (39).

It can be seen that the proposed DE-MOMI method, when compared to some other methods, gives quite good responses. The AH method for process G_{P5} gives somehow oscillatory response. For the same process, the ADRC method gives slightly oscillatory response during the reference change (see the process input signal). While DE_MOMI and MOMI methods clearly give the best tracking responses on process G_{P6}, all of the methods have similar disturbance-rejection performance. Only slightly oscillatory response can be observed for ADRC method.

For more objective comparison between the methods, the integral of absolute error (IAE) measure is used. The IAE value has been measured on tracking response (unity step-change of the reference r) and on disturbance rejection response (unity step-change of the process input disturbance d). The results are given in **Table 8**. It can be seen that the best values (marked with greyed colour) were obtained with DE-MOMI method.

The DE-MOMI method, therefore, compares favourably with few other methods, based on the non-parametric description of the process.

The process closed-loop responses for all the process models tested in this chapter (G_{P1} to G_{P6}) revealed that the proposed method can significantly improve the disturbance-rejection performance of the lower-order processes with smaller delays, while the improvement of the higher-order processes and/or processes with higher delays is not so significant. Therefore, the application of the method for lower-order processes with smaller delays might be beneficial in practice.

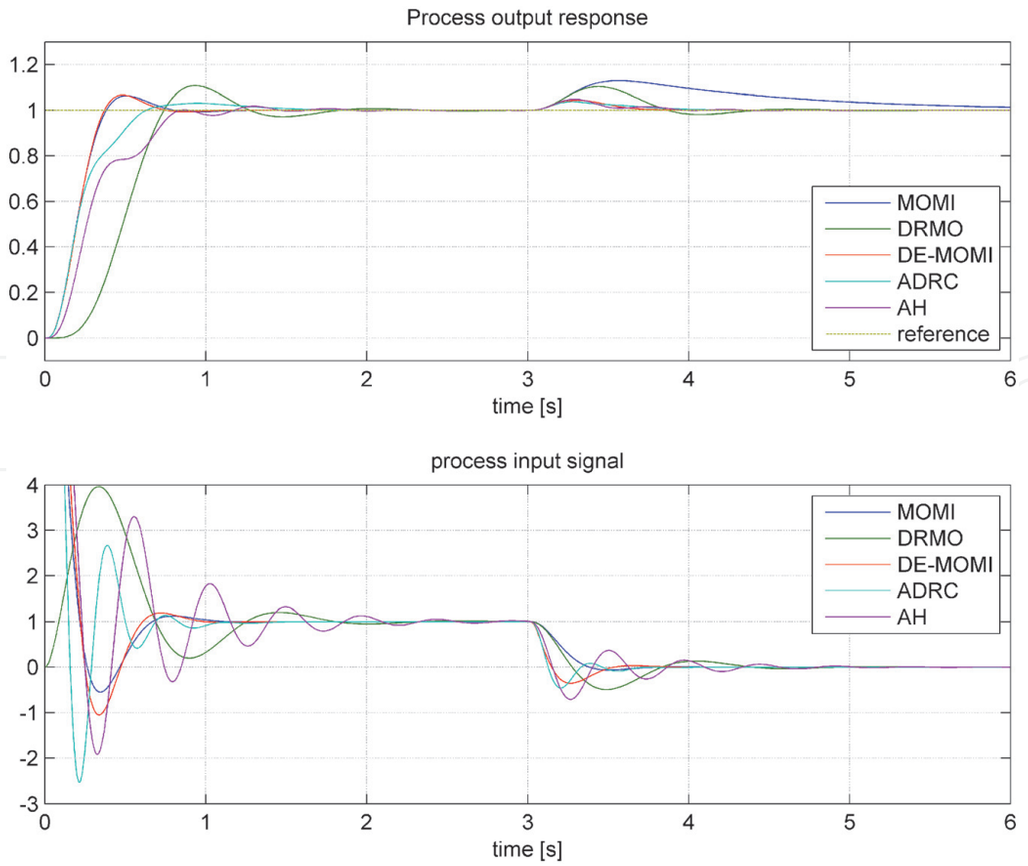


Figure 14.
The closed-loop responses on the process G_{P5}*, when using the MOMI, DRMO and DE-MOMI method.*

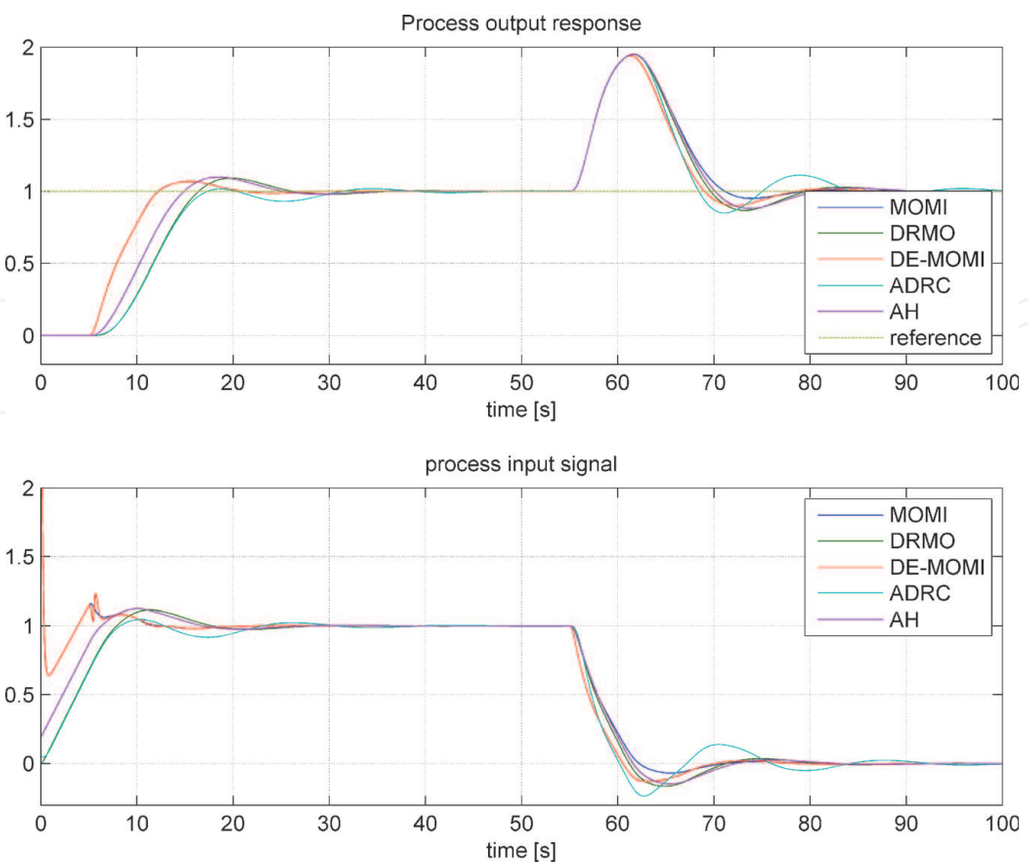


Figure 15.
The closed-loop responses on the process G_{P6}*, when using the MOMI, DRMO and DE-MOMI method.*

Process	experiment	DE-MOMI	MOMI	DRMO	AH	ADRC
G_{P5}	tracking	0.216	0.217	0.526	0.336	0.256
	DR	0.017	0.186	0.055	0.020	0.019
G_{P6}	tracking	8.66	8.66	12.34	11.06	12.32
	DR	7.80	8.42	8.79	8.89	8.83

Table 8.
The calculated IAE values for tracking and disturbance rejection (DR) responses for the processes (39).

7. Conclusions

In the chapter, it was shown that the disturbance rejection performance of the PID controller can be improved by adding a simple disturbance estimator (DE). The disturbance estimator consists of the process model and the inverse process model with DE filter. The advantage of the proposed approach is that the DE parameters can also be obtained directly from the nonparametric process data (time response of the process) without prior process identification. The same is true for the PID controller parameters, which are obtained using the MOMI tuning method. Of course, all PID and DE parameters can also be calculated from the process transfer function if it is known.

The proposed solution, called DE-MOMI method, has been tested on several different process models. It was shown that the control performance of the DE-MOMI method was significantly improved compared to similar MOMI and DRMO methods, especially for lower order processes with smaller time delays. In contrast, the improvements were noticeable but not as significant for higher order processes or processes with larger time delays. The additional advantage of the proposed method was that the tracking performance remained similar to that of the MOMI method.

The controller noise was controlled by the high frequency noise factors KPIDn and KDEn. The advantage of using these factors is that they can be easily understood and defined by the user.

The DE-MOMI method was also compared with some other non-parametric disturbance-rejection methods including the ADRC method. The results showed that the DE-MOMI method has either comparable or better control and tracking performance than the other tested methods. Nevertheless, it should be mentioned that the ADRC method uses a somewhat simpler control structure.

Future research activities could therefore focus on combining the advantages of the DE-MOMI and ADRC methods.

Acknowledgements

The authors gratefully acknowledge the contribution of the Ministry of Higher Education, Science and Technology of the Republic of Slovenia, Grant No. P2-0001 as well as the support by the grants APVV SK-IL-RD-18-0008 Platoon Modelling and Control for mixed autonomous and conventional vehicles: a laboratory experimental analysis and VEGA 1/0745/19 Control and modelling of mechatronic systems in emobility.

IntechOpen

IntechOpen

Author details

Damir Vrančić[1*] and Mikuláš Huba[2]

1 Jožef Stefan Institute, Department of Systems and Control, Ljubljana, Slovenia

2 Slovak University of Technology in Bratislava, Faculty of Electrical Engineering and Information Technology, Bratislava, Slovakia

*Address all correspondence to: damir.vrancic@ijs.si

IntechOpen

© 2021 The Author(s). Licensee IntechOpen. This chapter is distributed under the terms of the Creative Commons Attribution License (http://creativecommons.org/licenses/by/3.0), which permits unrestricted use, distribution, and reproduction in any medium, provided the original work is properly cited. CC BY

References

[1] Åström, K.J. and Hägglund, T. (1995). PID controllers: Theory, Design, and Tuning, 2nd Edition. Instrument Society of America.

[2] Åström, K.J., Panagopoulos, H. and Hägglund, T. (1998). Design of PI Controllers based on Non-Convex Optimization. Automatica, 34 (5), pp. 585–601.

[3] Garcia, C. E. and Morari, M. (1982). Internal model control. A unifying review and some new results. Ind. Eng. Chem. Process Des. Dev. Vol. 21, pp. 308–323.

[4] O'Dwyer A. (2009). Handbook of PI and PID controller tuning rules; 3rd Edition. Imperial College Press.

[5] Freire H., Moura Oliveira P., Solteiro E. P. and Bessa M., (2014), Many-Objective PSO PID Controller Tuning, Controlo 2014, Porto, Portugal pp. 183-192.

[6] Gorez, R. (1997). A survey of PID auto-tuning methods. Journal A. Vol. 38, No. 1, pp. 3–10.

[7] Kessler, C. (1955). Über die Vorausberechnung optimal abgestimmter Regelkreise Teil III. Die optimale Einstellung des Reglers nach dem Betragsoptimum. Regelungstechnik, Jahrg. 3, pp. 40–49.

[8] Taguchi, H. and Araki, M. (2000). Two-degree-of-freedom PID controllers – their functions and optimal tuning. Proceedings of the IFAC Workshop on Digital Control (PID'00), Terrassa, 2000. pp. 95–100.

[9] Vrančić, D. (2011) Magnitude optimum techniques for PID controllers. In: PANDA, Rames C. (editor). Introduction to PID controllers: theory, tuning and application to frontiers areas. Rijeka: InTech, cop., pp. 75–102.

[10] Whiteley, A. L. (1946). Theory of servo systems, with particular reference to stabilization. The Journal of IEE, Part II, 93(34), pp. 353–372.

[11] Vrančić D., Strmčnik S., and Hanus R. (2000). Magnitude optimum tuning using non-parametric data in the frequency domain. PID'00 : preprints : IFAC workshop on digital control: past, present and future of PID control, Terrassa, Spain, April 5-7, 2000, pp. 438–443.

[12] Vrančić, D., Strmčnik, S. and Juričić, Đ. (2001). A magnitude optimum multiple integration method for filtered PID controller. Automatica. Vol. 37, pp. 1473–1479.

[13] Ba Hli, F. (1954). A General Method for Time Domain Network Synthesis. IRE Transactions – Circuit Theory, 1 (3), pp. 21–28.

[14] Hanus, R. (1975). Determination of controllers parameters in the frequency domain. Journal A, XVI (3).

[15] Strejc, V. (1960). Auswertung der dynamischen Eigenschaften von Regelstrecken bei gemessenen Ein- und Ausgangssignalen allgemeiner Art. Z. Messen, Steuern, Regeln, 3(1), pp. 7–10

[16] Vrančić D. Strmčnik S., Kocijan J. and Moura Oliveira P. B. de. (2010). Improving disturbance rejection of PID controllers by means of the magnitude optimum method. ISA transactions, ISSN 0019–0578, vol. 49, no. 1, pp. 47–56.

[17] Vrančić D., Kocijan J. and Strmčnik S. (2004). Simplified disturbance rejection tuning method for PID controllers. ASCC The 5th Asian Control Conference, July 20–23, Melbourne, Australia. Conference proceedings.

[18] Vrančić D., Oliveira P.M., Cvejn J. (2017) The Model-Based Disturbance Rejection with MOMI Tuning Method for PID Controllers. In: Garrido P., Soares F., Moreira A. (eds) CONTROLO 2016. Lecture Notes in Electrical Engineering, Vol 402. Springer, Cham. https://doi.org/10.1007/978-3-319-43671-5_8.

[19] Vrančić D., Moura Oliveira P. and Huba M. (2018) "Optimizing Disturbance Rejection by Using Model-Based Compensator with User-Defined High-Frequency Gains," 13th APCA International Conference on Automatic Control and Soft Computing (CONTROLO), Ponta Delgada, 2018, pp. 330–335, doi: 10.1109/CONTROLO.2018.8514546.

[20] Moura Oliveira P., Vrančić D. and Freire H., (2014), Dual Mode Feedforward-Feedback Control System, Controlo 2014, Porto, Portugal pp. 241-50

[21] Preuss, H. P. (1991). Model-free PID-controller design by means of the method of gain optimum (in German). Automatisierungstechnik, Vol. 39, pp. 15–22.

[22] Rake, H. (1987). Identification: Transient- and frequency-response methods. In M. G. Singh (Ed.), Systems & control encyclopedia; Theory, technology, applications. Oxford: Pergamon Press.

[23] Vrečko D., Vrančić D., Juričić Đ. and Strmčnik S. (2001). A new modified Smith predictor: the concept, design and tuning. ISA transactions, ISSN 0019–0578, vol. 40, pp. 111–121.

[24] Huba, M. (2006). Constrained pole assignment control. Current Trends in Nonlinear Systems and Control, L. Menini, L. Zaccarian, Ch. T. Abdallah, Edts., Boston: Birkhäuser, pp. 163–183.

[25] Vrančić, D. (2020). Matlab/Octave function Octave_Calc_GC_GF.m for the calculation of controller and GE parameters based on a given filter time constants. Web page: https://octave-online.net/bucket~6UiDmdsr6yhSJs2MenYULF.

[26] Vrančić, D. (2020). Matlab/Octave function Octave_Calc_GC_GF_Noise.m for the calculation of controller and GE parameters based on a given noise gains. Web page: https://octave-online.net/bucket~Hofor19mDWWkAzZrhgeG7q.

[27] Chen X., Li D., Gao Z. and Wang C. (2011). Tuning Method for Second-order Active Disturbance Rejection Control. Proceedings of the 30th Chinese Control Conference, July 22–24, 2011, Yantai, China, Conference proceedings.

[28] Gao Z., Huang Y., and Han J. (2001). An Alternative Paradigm For Control System Design. Proceedings of the 40th IEEE Conference on Decision and Control, Orlando, USA, December 4-7, 2001, Vol. 5, doi: 10.1109/CDC.2001.980926, pp. 4578–4585.

[29] Han J. (2009). From PID to Active Disturbance Rejection Control. IEEE transactions on industrial electronics, ISSN 0278–0046, vol. 56, no. 3, pp. 900–906.

[30] Huba, M., Moura Oliveira P., Vrančić D., and Bistak P. (2019). ADRC as an exercise for modeling and control design in the state-space. 6th International Conference on Control, Decision and Information Technologies, CoDIt 2019, Paris, France April 23–26, 2019, pp. 464–469. doi: 10.1109/CoDIT.2019.8820543.

[31] Wang W. (2012). The New Design Strategy on PID Controllers. In: VAGIA, M. (editor). PID Controller Design Approaches, ISBN 978–953–51-6186-8, pp. 229–252.